Scientific Research Publishing

Journal of Environmental Protection, 2025, 16(3), 239-252
https://www.scirp.org/journal/jep
ISSN Online: 2152-2219
ISSN Print: 2152-2197

Study on the Photodegradation Mechanism of Sodium Diatrizoate in UV-Based Advanced Oxidation Processes

Yuying Wang*, Shuo Wang*, Runnan Liu*, Zhouna Li, Kunhui Liu#

College of Chemistry, Beijing Normal University, Beijing, China
Email: kunhui@bnu.edu.cn

How to cite this paper: Wang, Y.Y., Wang, S., Liu, R.N., Li, Z.N. and Liu, K.H. (2025) Study on the Photodegradation Mechanism of Sodium Diatrizoate in UV-Based Advanced Oxidation Processes. *Journal of Environmental Protection*, **16**, 239-252.
https://doi.org/10.4236/jep.2025.163012

Received: February 13, 2025
Accepted: March 10, 2025
Published: March 13, 2025

Abstract

Ultraviolet-based advanced oxidation processes (UV-AOPs) are techniques that utilize the synergistic action of ultraviolet light and oxidants to generate highly oxidative active radicals ($SO_4\bullet^-$, •OH, etc.) to degrade organic pollutants. Currently, research on degrading various pollutants using UV-AOPs mainly focuses on degradation efficiency, toxic by-products, and mineralization rate. However, studies are limited on how the photochemical reactions of organic pollutants that absorb ultraviolet light themselves affect the advanced oxidation degradation process. As one of refractory pharmaceutical and personal care products (PPCPs), the ionic contrast agent sodium diatrizoate (DTZ) has excellent ultraviolet absorption, but there are no reports on how its optical behavior influences the photo-oxidative degradation process. In this study, spectroscopic techniques were employed to investigate the photodegradation pathways of DTZ under different wavelengths. It was found that under UVC irradiation, DTZ undergoes a deiodination pathway to form DTZ-I, which in turn affects the target of photoactivated generation of active radicals ($SO_4\bullet^-$), leading to a DTZ advanced oxidation degradation pathway different from that under UVA irradiation. These results provide theoretical support and research insights for understanding the degradation processes of pollutants that can directly undergo photoreactions with ultraviolet light in UV based advanced oxidation processes.

Keywords

Sodium Diatrizoate, UV-Based Advanced Oxidation Processes, Reactive Radicals, Degradation Pathway

---

*Equally contributed.
#Corresponding author.

1. Introduction

Iodinated X-ray contrast media (ICMs) are indispensable agents in medical diagnostics, extensively utilized for imaging soft tissues and internal organs. The chemical structures and properties of iodinated contrast agents are highly stable, rendering them resistant to degradation and classifying them as persistent pharmaceutical and personal care products (PPCPs) [1]-[4]. Among these, sodium diatrizoate (DTZ) stands out as a representative ionic contrast agent. As shown in **Figure 1**, the free carboxyl group on the phenyl ring side chain imparts high polarity and robust biological and chemical stability to DTZ, leading to its prolonged accumulation in aquatic environments [5]-[9]. Furthermore, DTZ can degrade into secondary pollutants such as absorbable organic halogens (AOX) and iodinated disinfection by-products (I-DBPs) [10]-[12], posing irreversible threats to mammalian health.

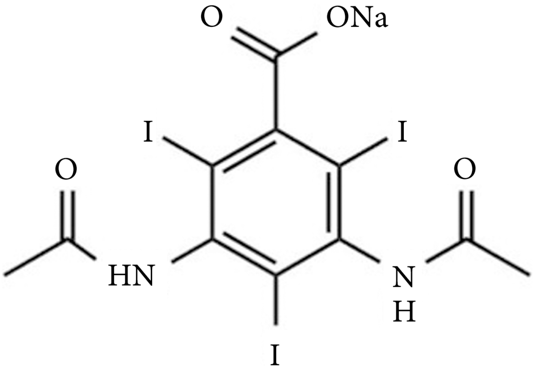

Figure 1. Structural formula of sodium diatrizoate (DTZ).

Extensive research has been conducted on the degradation of DTZ in aquatic environments [13] [22]. While ionizing radiation techniques have demonstrated high degradation efficiency, they often exhibit low mineralization capacity, typically breaking down pollutants into disinfection by-products and other secondary pollutants [13]. Norman Hack and colleagues reported a biological treatment method; however, the degradation rate was relatively slow [14] [15]. Additionally, studies have indicated that nitrifying bacteria or anaerobic bacteria possess the ability to degrade iodinated contrast agents, though these methods still have room for improvement in degradation efficiency and process precision [13] [16]-[21]. In recent years, direct UV degradation of pollutants has gained favor due to its efficiency and the absence of secondary pollution. However, Allard *et al.* found that the iodinated by-products generated during the photodegradation of contrast agents increase with enhanced UV light exposure [22]. Xiang and colleagues demonstrated that advanced oxidation processes (AOPs) [23], which utilize highly reactive and oxidative radicals (such as $SO_4^{\bullet-}$ and $\bullet OH$) to attack the stable structures of pollutants, effectively transform refractory organic pollutants into carbon dioxide, water, inorganic salts, and other small molecules [24]. Meanwhile, Manuel Sánchez-Polo *et al.*, demonstrated that the UV/$K_2S_2O_8$ system exhibits superior degradation efficiency for DTZ compared to other advanced oxidation processes, such as the Fenton process [25]. Introducing UV light into these technologies enhances the photolysis of oxidants, producing a substantial amount of active radicals, thereby more effectively degrading emerging pollutants. Previous studies on the UV photolysis of oxidants generating active radicals for DTZ degradation have primarily focused on improving degradation efficiency and mineralization rates, as well as detecting various stable products to assess reaction safety and infer possible degradation pathways [24]. However, research has shown that certain contrast agents undergo deiodination under UV exposure, forming stable deiodinated products [26]-[28]. This raises the question of whether DTZ also undergoes similar deiodination and generates corresponding deiodinated products. If deiodination occurs, it is crucial to determine whether active radicals primarily attack DTZ itself or its photo transformed products. These issues have been scarcely discussed in the literature but are vital for understanding the degradation mechanisms of DTZ in UV-AOPs [29].

In this study, we employed ultraviolet light of varying wavelengths to activate oxidants such as sodium persulfate (PS) and hydrogen peroxide (H_2O_2), generating highly reactive radicals ($SO_4•^-$ and •OH) to degrade DTZ. By monitoring changes in absorption spectra, we investigated the photodegradation pathways of DTZ. Notably, we observed that under UV light exposure, DTZ exhibits deiodination behavior, leading to a shift in the primary target of active radicals and resulting in two distinct degradation pathways. These findings not only enhance our understanding of DTZ degradation behavior but also provide theoretical insights for applying UV-based advanced oxidation technologies to treat photosensitive pollutants in wastewater treatment [23] [24].

2. Materials and Methods

2.1. Materials

The reagents used in this study are listed in **Table 1**. All reagents were purchased without further purification and used directly in the experiments. High-purity water was obtained using a Millipore purification system.

Table 1. Reagents used in current experiments.

Reagent	Purity	Supplier
Sodium Diatrizoate ($C_{11}H_8I_3N_2NaO_4$, DTZ)	≥98%	Shanghai Yuanye Biotechnology Co., Ltd.
Hydrogen Peroxide (H_2O_2)	30%	Tongguang Fine Chemicals Co., Ltd.
Sodium Persulfate ($Na_2S_2O_8$, PS)	≥99%	Shanghai Macklin Biochemical Technology Co., Ltd.

2.2. Experimental Methods

Steady-State UV-Visible Absorption Spectroscopy: In this study, steady-state UV-visible absorption spectra were acquired using a Hitachi U-3900 UV-Visible spectrophotometer. The scanning speed was set at 600 nm/min, with ultrapure water as the background. Spectra were collected in the wavelength range of 200 – 600 nm at room temperature.

Theoretical Computational Methods: Gaussian 09 software was employed for theoretical calculations at the B3LYP level of theory. The 6-31G* basis set was used for most atoms, while the Stuttgart-Dresden (SDD) basis set was applied for iodine atoms. Optimized geometries of the deiodinated analogs of diatrizoate (DTZ) were calculated, and time-dependent density functional theory (TD-DFT) was utilized to compute their absorption spectra. The Polarizable Continuum Model (PCM) was applied to simulate the solvent effect of water.

3. Results and Discussion

3.1. Effect of UV-Based Advanced Oxidation Processes on the Degradation Efficiency of Sodium Diatrizoate

In the field of environmental pollutant remediation, advanced oxidation processes (AOPs) based on hydroxyl radicals (•OH) and sulfate radicals ($SO_4{\bullet}^-$), particularly UV/H_2O_2 and UV/$Na_2S_2O_8$ (PS) degradation systems, have been widely applied to degrade persistent organic pollutants in the environment.

In this study, we first investigated the degradation of sodium diatrizoate (DTZ) in advanced oxidation processes. The UV-visible absorption spectrum of DTZ is shown in Figure 2(a), with a maximum absorption peak at 236 nm. Therefore, we evaluated the degradation efficiency of DTZ by monitoring the change in absorbance at 236 nm, calculated using the formula 1-C/C_0. In the preliminary experiments, we screened the experimental conditions based on spectral absorbance and degradation effects, and then set up six optimized control experiments, including: 50 μM DTZ, 50 μM DTZ + 4 mM PS, 50 μM DTZ + 4 mM H_2O_2, 50 μM DTZ + 254 nm UV, and 50 μM DTZ + 4 mM PS/H_2O_2 + 254 nm UV. The degradation period was observed for 3 hours, with UV absorption spectra of the mixed solutions measured every half hour. The degradation results are shown in Figure 2(b).

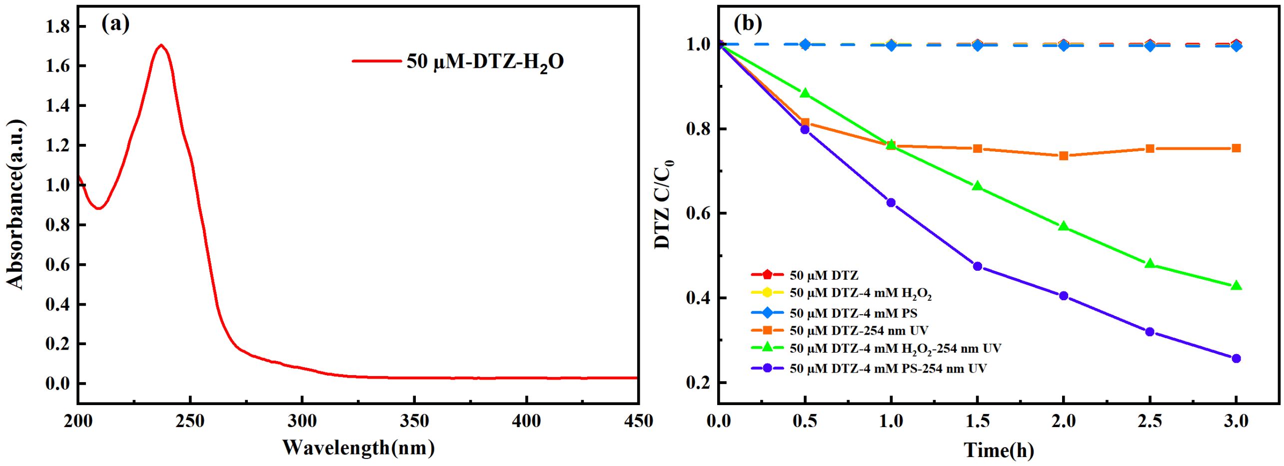

Figure 2. (a) UV-Vis absorption spectra of 50 μM DTZ, (b) Degradation of DTZ in different systems.

From Figure 2(b), it is obvious that in the system without 254 nm UV light, DTZ was almost not degraded. When 254 nm UV light was used alone, DTZ began to show slight degradation, indicating that 254 nm UV light has some degradation effect on DTZ. Further introduction of hydrogen peroxide (H_2O_2) and sodium persulfate (PS) as oxidants into the 254 nm UV light system significantly improved the degradation efficiency of DTZ, suggesting the key role of active radicals in the degradation process. Notably, when using PS as the oxidant, the degradation rate of DTZ was significantly faster than that in the H_2O_2 system. This experimental result further indicates that, compared to hydroxyl radicals (•OH), sulfate radicals ($SO_4^{\bullet-}$) exhibit superior effectiveness in degrading DTZ. The reaction processes of UV photolysis of oxidants are shown in equations (1) and (2).

$$H_2O_2 \xrightarrow{h\upsilon} 2\bullet OH \tag{1}$$

$$S_2O_8^{\ 2-} \xrightarrow{h\upsilon} 2SO_4^{\ \bullet-} \tag{2}$$

M. Sprehe *et al.* observed deiodination behavior of non-ionic contrast agents (iopromide and iopamidol) during photochemical oxidation reactions [28]. Tao Ye *et al.* also emphasized the presence of deiodination behavior of iodinated contrast agents (ICMs) under UV light, leading to the formation and accumulation of iodinated disinfection by-products (I-DBPs) in aquatic environments [30]. These studies raise a key question: Does the photoreaction process of DTZ also exhibit deiodination behavior? Does the main target of active radicals in the UV photolysis oxidation process of oxidants change due to deiodination behavior? To explore these issues, we conducted systematic analysis and interpretation by introducing UV light of different wavelengths, aiming to reveal the impact of UV light on the molecular structure of DTZ and the specific mechanisms of free radicals in the degradation process.

3.2. Influence of Different Wavelengths of Ultraviolet Light on the Photoreaction Process of Sodium Diatrizoate

The molecular structure of a substance imparts unique absorption characteristics, which are crucial in studies involving the photodegradation of pollutants under ultraviolet (UV) light. Therefore, selecting appropriate UV wavelengths is a key factor when exploring the impact of UV light on pollutant degradation. As shown in **Figure 2(a)**, sodium diatrizoate (DTZ) exhibits significant absorption below 300 nm and minimal absorption above 300 nm. Therefore, we conducted comparative experiments using UV light at wavelengths where DTZ has substantial absorption (254 nm and 266 nm) and at wavelengths where it has minimal absorption (355 nm and 365 nm) to investigate whether DTZ undergoes deiodination and to elucidate the specific mechanisms of free radicals in the reaction. By observing and comparing the effects of different UV wavelengths on the degradation process of sodium diatrizoate, we aimed to uncover the involved reaction mechanisms.

As depicted in **Figure 3(a)**, under 254 nm UVC irradiation, the maximum absorption wavelength of DTZ shifted from 236 nm to 225 nm over time, accompanied by an increase in absorbance at 225 nm. Additionally, weak absorption appeared in the 275 - 350 nm range. This phenomenon indicates that under UVC

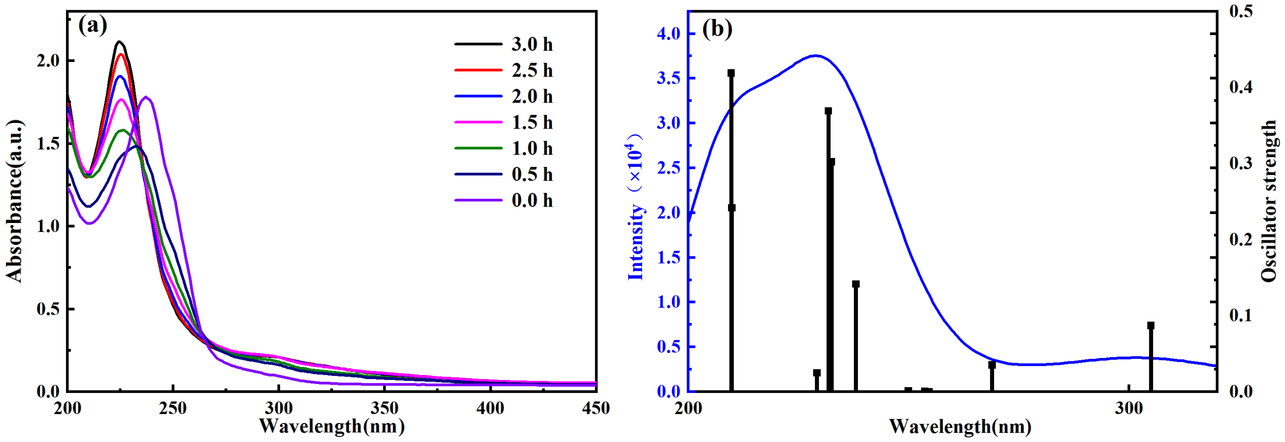

Figure 3. (a) Spectral evolution of 50 μM DTZ under 254 nm UV irradiation, (b) UV absorption spectra of DTZ-I substances calculated at the level of PCM/B3LYP/6-31G*.

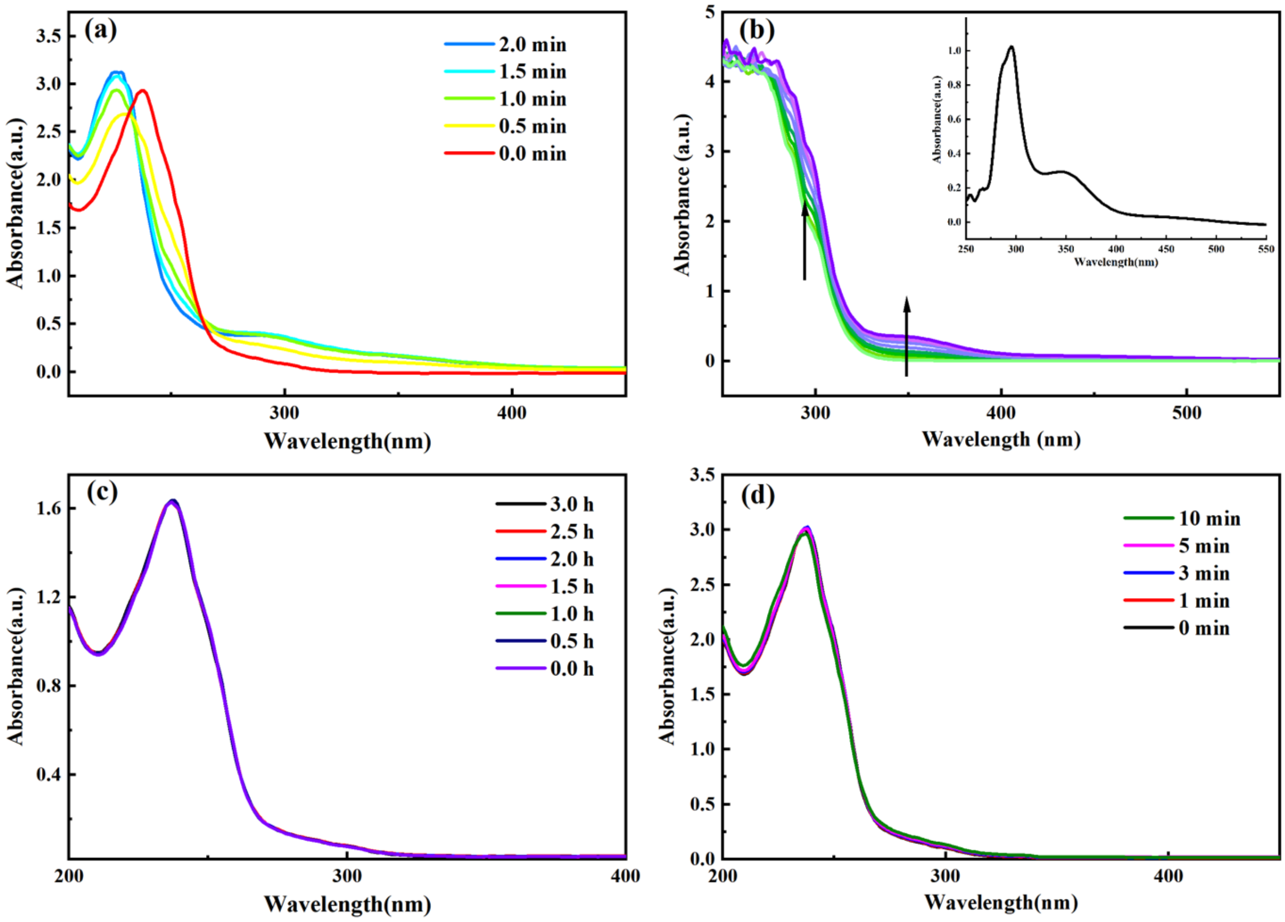

Figure 4. (a) Spectral evolution of 100 μM DTZ under 266 nm laser irradiation; (b) Evolution of UV absorption spectra of 1 mM DTZ during irradiation, where the inset shows the difference spectrum of UV-vis absorption spectra before and after 2 min of light exposure to 1 mM DTZ; (c) Spectral evolution of DTZ under 365 nm UV irradiation; (d) Spectral evolution of DTZ under 355 nm laser irradiation Laser wavelength: 266 nm; laser energy: 10 mJ.

irradiation, the structure of DTZ undergoes transformation. According to literature reports, UV absorption due to C-I bonds occurs around 240 – 245 nm, with a molar extinction coefficient of approximately 3×10^4 $M^{-1} \cdot cm^{-1}$ [28]-[30]. Therefore, when the C-I bond breaks, a significant decrease in the extinction coefficient and a shift of the absorption spectrum to shorter wavelengths are observed.

Based on these observations and literature evidence, we hypothesize that under 254 nm UVC irradiation, DTZ undergoes deiodination to form a deiodinated analog (hereafter referred to as DTZ-I).

To further explain this phenomenon, we performed time-dependent density functional theory (TD-DFT) calculations to obtain the UV absorption spectrum of the DTZ deiodinated analog (**Figure 3(b)**). The calculated spectrum closely matches the experimental observations in **Figure 3(a)**, with a maximum absorption wavelength at 225 nm and weak absorption features in the 275 – 350 nm range, confirming that under 254 nm UVC irradiation, DTZ undergoes structural transformation to form the deiodinated analog DTZ-I. In order to capture the spectral evolution of DTZ more rapidly under UVC irradiation, we employed a higher energy density 266 nm UVC laser to irradiate a higher concentration of DTZ. As shown in **Figure 4(a)**, when a 100 μM DTZ solution was irradiated with a 266 nm laser, the spectral evolution within 2 minutes of laser irradiation exhibited the same trend as the 3-hour reaction under 254 nm UVC irradiation: the maximum absorption peak shifted from 236 nm to 225 nm, accompanied by an increase in absorbance. Furthermore, we increased the DTZ concentration to 1 mM and continued irradiation with the 266 nm laser. As shown in **Figure 4(b)**, during this process, we observed a significant increase in absorbance at 288 nm and 350 nm, and the solution color turned yellow (**Figure 5(a)**, right). This further indicates that new substances were generated during the 266 nm UVC irradiation of DTZ. These substances could turn colorless potassium iodide-starch paper blue (**Figure 5(b)**, right). The inset in **Figure 4(b)** reveals that approximately 2 minutes after laser irradiation, new substances were produced. Combining experimental results and literature reports, we attribute these new substances to the triiodide anion I_3^- [31].

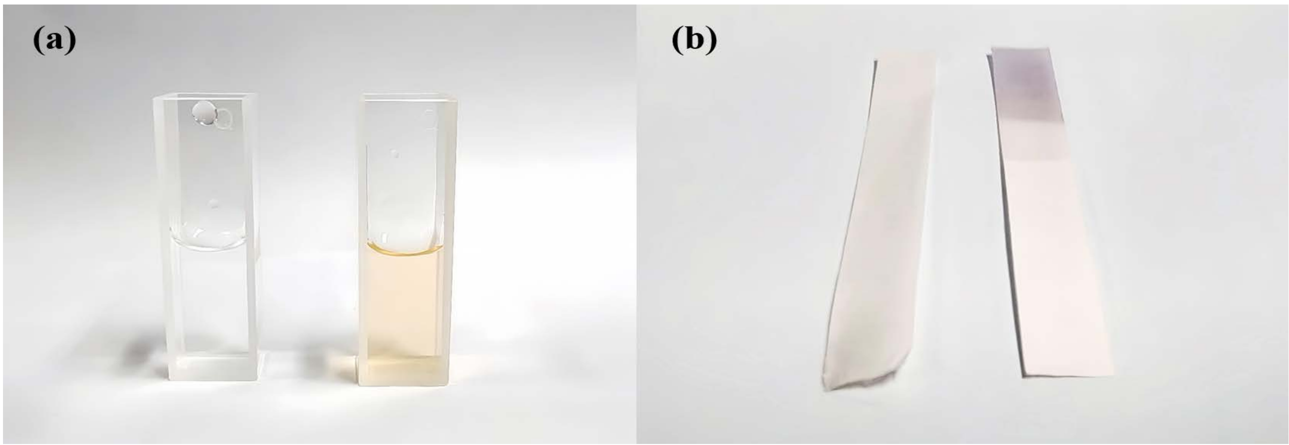

Figure 5. (a) Color change of 1 mM DTZ before (left) and after (right) laser irradiation at 266 nm; (b) Experimental phenomena observed with potassium iodide starch test paper before (left) and after (right) laser irradiation at 266 nm; laser wavelength: 266 nm; laser energy: 10 mJ.

These experimental results suggest that under UV light wavelengths where DTZ has substantial absorption (254 nm and 266 nm), DTZ molecules tend to undergo deiodination, forming triiodide anions I_3^- and the deiodinated analog DTZ-I. Subsequently, we irradiated DTZ with UV light at wavelengths where it has minimal absorption (355 nm and 365 nm) and observed the spectral evolution (**Figure 4(c)-(d)**). The results showed that under 355 nm and 365 nm UVA irradiation, the UV absorption spectrum of DTZ did not undergo significant changes, indicating that under UVA irradiation, the molecular structure of DTZ remains stable without deiodination.

By introducing UV light of different wavelengths, we found that DTZ undergoes different photoreaction processes. Under UV light wavelengths where it has substantial absorption (254 nm and 266 nm), DTZ first undergoes C-I bond cleavage, generating triiodide anions I_3^- and the deiodinated analog DTZ-I. Under UV light wavelengths where it has minimal absorption (355 nm and 365 nm), DTZ undergoes minimal photoreaction. Therefore, the essence of DTZ's photoreaction is closely related to its own UV absorption characteristics. Thus, when studying the photoreaction behavior of such substances, it is essential to pay particular attention to their inherent properties. Moreover, as the energy density of UV light increases, the photoreaction rate of DTZ accelerates, allowing the molecular structural evolution to be observed over a shorter period using spectroscopic techniques. These findings further confirm the significant impact of UV light wavelength and energy on the degradation behavior of organic pollutants and provide a reasonable perspective for understanding the mechanisms of UV light in pollutant treatment processes.

3.3. Mechanism of Active Free Radicals in the Degradation of Sodium Diatrizoate

Based on the previous studies, we observed significant differences in the photoreaction processes of sodium diatrizoate (DTZ) under different wavelengths of ultraviolet (UV) light. This observation raises an important question: what is the specific role of active free radicals in the photodegradation of DTZ within advanced oxidation processes? To address this question, we designed a series of comparative experiments combining the oxidant sodium persulfate (PS) with UV light of varying wavelengths. Actually, we performed experiments using peroxymonosulfate (PDS) as an oxidant for DTZ degradation, and the results demonstrated a satisfactory degradation effect. However, compared to sodium persulfate upon decomposition produces solely sulfate radicals ($SO_4{\bullet}^-$), PDS generates both $SO_4{\bullet}^-$ and hydroxyl radicals (•OH), which may lead to competitive reactions between $SO_4{\bullet}^-$ and •OH with DTZ, thereby complicating the reaction system. This approach by PS allowed us to better observe the key role of sulfate radicals ($SO_4{\bullet}^-$), which possess high reactivity and strong oxidative capabilities, in the efficient degradation of DTZ.

As shown in **Figure 6(a)**, in the system where 365 nm UVA UV light activates the oxidant PS, DTZ undergoes some degradation. Considering the findings from

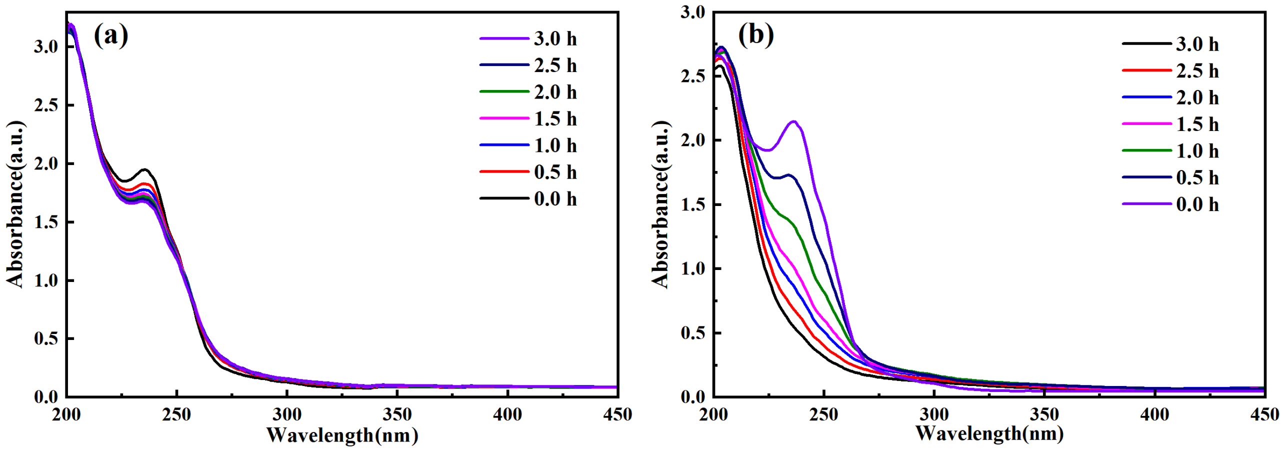

Figure 6. (a) Evolution of UV-Vis absorption spectra of DTZ/PS system under irradiation with 365 nm UV light, (b) 254 nm UV light.

previous sections, where 365 nm UV light does not affect the molecular structure of DTZ, we conclude that 365 nm UVA UV light can photolyze PS to generate sulfate radicals, which then degrade DTZ. The degradation pathway under UVA UV light is proposed as shown in Equation (3).

$$\mathrm{DTZ} + \mathrm{SO}_4^{\bullet -} \rightarrow \text{product} \tag{3}$$

Subsequently, we introduced 254 nm UVC UV light into the DTZ degradation system with PS as the oxidant. We observed rapid degradation of DTZ under 254 nm UV light. What is the degradation pathway for this process? Given that DTZ exhibits its own photochemical deiodination behavior at this wavelength, does this affect the primary target of $SO_4^{\bullet -}$? We then varied the concentration of PS to control the amount of $SO_4^{\bullet -}$ in the system. By observing the degradation extent of the pollutant corresponding to different concentrations of $SO_4^{\bullet -}$, we inferred the main target of the free radicals and the overall degradation pathway.

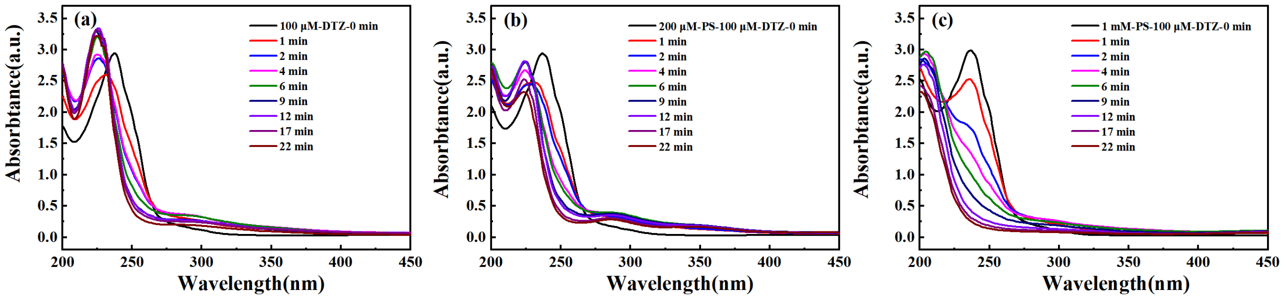

Figure 7. Evolution of UV-visible absorption spectra of the system during laser irradiation; laser wavelength: 266 nm; laser energy: 40 mJ. (a) DTZ; (b) DTZ/200 μM PS; (c) DTZ/1 mM PS.

We irradiated 100 μM DTZ, 200 μM PS + 100 μM DTZ, and 1 mM PS + 100 μM DTZ systems with 266 nm UVC laser light and observed the spectral evolution in these systems. As shown in Figure 7(a), under 266 nm laser irradiation, the absorption spectrum of DTZ blue-shifts, and its structure undergoes significant changes, consistent with our findings in Section 3.1. In this system, we further introduced different concentrations of PS to generate $SO_4^{\bullet-}$ for DTZ degradation, as shown in Figure 7(b) and Figure 7(c). When the initial concentration of PS in the system was 200 μM, the reaction rate of DTZ was slower, and the entire absorption spectrum exhibited a blue-shift, consistent with the changes observed in DTZ under 266 nm laser irradiation. However, when the initial concentration of PS was 1 mM, the reaction rate of DTZ was faster, and the intermediate reaction process was hardly observable, further indicating that the amount of $SO_4^{\bullet-}$ in the system significantly impacts the degradation process of DTZ.

To further distinguish the primary target of $SO_4^{\bullet-}$ and the degradation pathway of DTZ under 266 nm UVC UV light, we performed differential spectral analysis on the spectra of different systems at various time points. Differential spectra at different times (subtracting the UV spectrum of the 200 μM PS + 100 μM DTZ degradation system from that of the 100 μM DTZ reaction system) are shown in Figure 8(a). We can clearly observe that after introducing $SO_4^{\bullet-}$ into the system, the molecular structure of DTZ first undergoes a transformation, with the maximum absorption wavelength shifting from 236 nm to below 230 nm, followed by a decrease in absorbance at this maximum wavelength. Next, we subtracted the UV spectra of the 1 mM PS + 100 μM DTZ degradation system from those of the 200 μM PS + 100 μM DTZ degradation system, as shown in Figure 8(b). We can clearly see that when the amount of $SO_4^{\bullet-}$ differs, the degradation system with a higher concentration of $SO_4^{\bullet-}$ degrades more of the pollutant, and this pollutant has a maximum absorption wavelength around 225 nm, with regular changes over time (the maximum negative peak in Figure 8(b) is at 225 nm). These experimental results indicate that under 266 nm UVC UV light, DTZ first tends to undergo structural transformation to generate DTZ-I, and $SO_4^{\bullet-}$ primarily reacts with DTZ-I. Therefore, the degradation pathways of DTZ are proposed as shown in Equations (4) and (5).

$$\text{DTZ} \overset{\text{UVC}}{\rightarrow} \text{DTZ-I} \tag{4}$$

$$\text{DTZ-I} + \text{SO}_4^{\bullet-} \rightarrow \text{product} \tag{5}$$

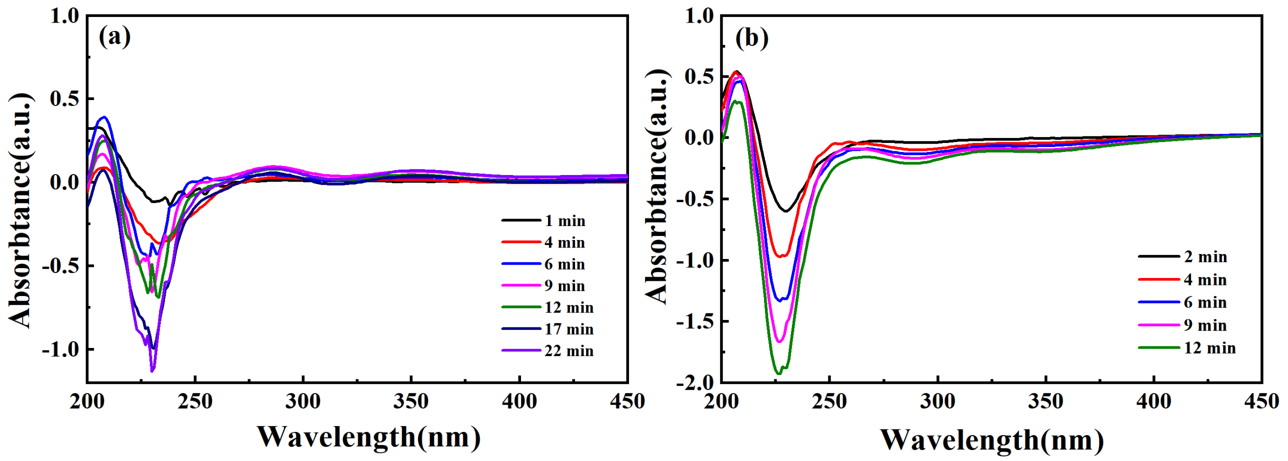

Figure 8. (a) Differential spectra of DTZ system and DTZ/200 μM PS system (*i.e.*, Figure 7(a)-(b)); (b) Differential spectra of DTZ/200 μM PS system and DTZ/1 mM PS system (*i.e.*, Figure 7(c)-(b)); laser wavelength: 266 nm; laser energy: 40 mJ.

These findings clearly indicate that under UVA light irradiation, $SO_4^{\bullet -}$ primarily reacts with DTZ itself, whereas under UVC light irradiation, $SO_4^{\bullet -}$ primarily reacts with the deiodinated product DTZ-I. These observations not only align with the effects of different wavelengths of UV light on the photoreaction process of DTZ but also further confirm the close relationship between the photochemical properties of DTZ and its degradation behavior. This study enhances our understanding of the mechanisms of UV-based advanced oxidation processes (UV-AOPs) in the degradation of DTZ, elucidating the key degradation role of highly reactive $SO_4^{\bullet -}$ under different wavelengths of UV light and its specific interactions with the DTZ molecule or its deiodinated product DTZ-I. These insights not only enrich the existing literature but also provide a solid data foundation and theoretical support for the development of degradation strategies targeting contrast agents and the exploration of reaction mechanisms.

4. Conclusion

In this study, we conducted an in-depth investigation into the degradation process of sodium diatrizoate (DTZ) in UV-based advanced oxidation processes (UV-AOPs) using ultraviolet-visible (UV-Vis) absorption spectroscopy, specific wavelength UV light, and theoretical calculations. Our findings reveal significant differences in the photoreaction processes of DTZ under various UV wavelengths. Under UVC exposure, the C-I bond in DTZ undergoes cleavage, resulting in the formation of the deiodinated analog DTZ-I. Conversely, UVA does not induce structural changes in DTZ. Consequently, in systems exposed to different UV wavelengths, the reactive radicals in the advanced oxidation process primarily target different components, leading to distinct degradation pathways. Under UVA exposure, since the C-I bond in DTZ remains intact, DTZ itself becomes the main target for reactive radicals. Under UVC exposure, DTZ undergoes deiodination, and reactive radicals primarily interact with the deiodinated analog DTZ-I. This study not only fills the gap in the existing literature regarding the unique role of UV light in the degradation of DTZ during UV-AOPs but also provides a reasonable research approach for the degradation processes of similar pollutants susceptible to UV light.

Conflicts of Interest

The authors declare no conflicts of interest regarding the publication of this paper.

References

[1] Chen, H.B., Cheng, X.Y., Ye, X.F., He, H., Gao, Z.Q., Peng, Y., Hu, G.J., Yang, S.G., Li, S.Y. and Zhang, L.M. (2019) Research Progress on the Analytical Methods and Pollution Status of Iodinated X-Ray Contrast Media. *Environmental Chemistry*, **38**, 1919-1929.

[2] Yang, H.Y., Li, X.L., Wang, Z., Chen, L., Kong, Y. and Zheng, X. (2021) Research Progress on the Environment Concentration, Analytical Methods and Toxicity Evaluation of Iodinated X-Ray Contrast Medias. *Environmental Chemistry*, **40**, 141-149.

[3] Li, X., Hu, X.L. and Yin, D.Q. (2015) Review: Occurrence of Iodinated X-Ray Contrast Media and Their Removal Processes in the Aquatic Environment. *Environmental Chemistry*, **34**, 555-564.

[4] Sanderson, H., Dyer, S.D. and Price, B.B. (2006) Occurrence and Weight-of-Evidence Risk Assessment of Alkyl Sulfates, Alkyl Ethoxysulfates, and Linear Alkylbenzene Sulfonates (LAS) in River Water and Sediments. *Science of the Total Environment*, **368**, 695-712. https://doi.org/10.1016/j.scitotenv.2006.04.030

[5] Watkinson, A.J., Murby, E.J., Kolpin, D.W. and Costanzo, S.D. (2009) The Occurrence of Antibiotics in an Urban Watershed: From Wastewater to Drinking Water. *Science of the Total Environment*, **407**, 2711-2723. https://doi.org/10.1016/j.scitotenv.2008.11.059

[6] Ding, S.Y., Niu, J.F. and Bao, Y.P. (2013) Evidence of Superoxide Radical Contribution to Demineralization of Sulfamethoxazole by Visible-Light-Driven $Bi_2O_3/Bi_2O_2Co_3/Sr_6Bi_2O_9$ Photocatalyst. *Journal of Hazardous Materials*, **262**, 812-818. https://doi.org/10.1016/j.jhazmat.2013.09.048

[7] Klavarioti, M., Mantzavinos, D. and Kassinos, D. (2009) Removal of Residual Pharmaceuticals from Aqueous Systems by Advanced Oxidation Processes. *Environment International*, **35**, 402-417. https://doi.org/10.1016/j.envint.2008.07.009

[8] Xu, W.H., Zhang, G. and Zou, S.C. (2007) Determination of Selected Antibiotics in the Victoria Harbour and the Pearl River, South China Using High-Performance Liquid Chromatography-Electrospray Ionization Tandem Mass Spectrometry. *Environmental Pollution*, **145**, 672-679. https://doi.org/10.1016/j.envpol.2006.05.038

[9] Garcia-Galan, M.J., Diaz-Cruz, M.S. and Barcelo, D. (2011) Occurrence of Sulfonamide Residues along the Ebro River Basin: Removal in Wastewater Treatment Plants and Environmental Impact Assessment. *Environmental Pollution*, **37**, 462-473. https://doi.org/10.1016/j.envint.2010.11.011

[10] Dong, H.Y., Qiang Z.M. and Lian, J.F. (2018) Deiodination of Iopamidol by Zero Valent Iron (ZVI) Enhances Formation of Iodinated Disinfection By-Products during Chloramination. *Water Research*, **129**, 319-326. https://doi.org/10.1016/j.watres.2017.11.032

[11] Wei, H., Hao, M. and Li, J. (2021) The Oxidation Performance and Intermidates Toxicity of Sodium Diatrizoate in the Ultrasound Activated Peroxymonosulfate System. *Acta Scientiae Circumstantiae*, **41**, 4538-4546.

[12] Hu, C.Y., Xu, L. and Lin, Y.L. (2024) A Comparative Study on the Degradation of Iohexol and Diatrizoate during UV/Persulfate Process: Kinetics, Degradation Pathways and Iodinated Disinfection By-Products. *Environmental Science: Water Research & Technology*, **10**, 718-728. https://doi.org/10.1039/D3EW00696D

[13] Velo-Gala, I., López-Peñalver, J.J. and Sánchez-Polo, M. (2012) Ionic X-Ray Contrast Media Degradation in Aqueous Solution Induced by Gamma Radiation. *Chemical Engineering Journal*, **195**-**196**, 369-376. https://doi.org/10.1016/j.cej.2012.04.046

[14] Hack, N., Reinwand, C. and Abbt-Braun, G. (2015) Biodegradation of Phenol, Salicylic Acid, Benzenesulfonic Acid, and Iomeprol by *Pseudomonas* Fluorescens in the Capillary Fringe. *Journal of Contaminant Hydrology*, **183**, 40-54. https://doi.org/10.1016/j.jconhyd.2015.10.005

[15] Zhang, W., Soutrel, I. and Amrane, A. (2022) Improvement of the Biodegradability of Diatrizoate by Electroreduction of Its Amido Groups. *Separation and Purification Technology*, **285**, Article 120317. https://doi.org/10.1016/j.seppur.2021.120317

[16] Liu, Y., Hu, J. and Xu, B. (2013) Isolation and Identification of an Iopromide-Degrading Strain and Its Application in an A^2/O System. *Bioresource Technology*, **134**,

36-42. https://doi.org/10.1016/j.biortech.2013.02.043

[17] Xu, B.J., Gao, P. and Liu, Z.H. (2014) Influence of Cosubstrates on Iopromide Degradation by *Pseudomonas* sp. I-24. *Water Air & Soil Pollution*, **225**, Article No. 1849. https://doi.org/10.1007/s11270-013-1849-x

[18] Babbitt, C.W., Pacheco, A. and Lindner, A.S. (2009) Methanol Removal Efficiency and Bacterial Diversity of an Activated Carbon Biofilter. *Bioresource Technology*, **100**, 6207-6216. https://doi.org/10.1016/j.biortech.2009.06.110

[19] Lecouturier, D., Rochex, A. and Lebeault, J.M. (2008) The Mineralization of 5-Amino-2,4,6-Triiodoisophthalic Acid by a Two-Stage Fixed-Bed Reactor. *Water Research*, **42**, 2491-2498. https://doi.org/10.1016/j.watres.2008.02.006

[20] Kalsch, W. (1999) Biodegradation of the Iodinated X-Ray Contrast Media Diatrizoate and Iopromide. *Science of the Total Environment*, **225**, 143-153. https://doi.org/10.1016/S0048-9697(98)00340-4

[21] Hapeshi, E., Lambrianides, A. and Koutsoftas, P. (2013) Investigating the Fate of Iodinated X-Ray Contrast Media Iohexol and Diatrizoate during Microbial Degradation in an MBBR System Treating Urban Wastewater. *Environmental Science and Pollution Research*, **20**, 3592-3606. https://doi.org/10.1007/s11356-013-1605-1

[22] Allard, S., Criquet, J. and Prunier, A. (2016) Photodecomposition of Iodinated Contrast Media and Subsequent Formation of Toxic Iodinated Moieties during Final Disinfection with Chlorinated Oxidants. *Water Research*, **103**, 453-461. https://doi.org/10.1016/j.watres.2016.07.050

[23] Saeid, S., Tolvanen, P. and Kumar, N. (2018) Advanced Oxidation Process for the Removal of Ibuprofen from Aqueous Solution: A Non-Catalytic and Catalytic Ozonation Study in a Semi-Batch Reactor. *Applied Catalysis B*: *Environmental*, **230**, 77-90. https://doi.org/10.1016/j.apcatb.2018.02.021

[24] Xiang, W.M., Yang, S.G., Sun, D.Y., Ji, Q.Y., Zhou, W., Xu, C.M., He, H. and Li, S.Y. (2022) Research Progress of Advanced Oxidation Technology to Remove Iodine X-ray Contrast Media in Water. *Environmental Chemistry*, **41**, 260-275.

[25] Velo-Gala, I., López-Peñalver, J.J., Sánchez-Polo, M. and Rivera-Utrilla, J. (2014) Comparative Study of Oxidative Degradation of Sodium Diatrizoate in Aqueous Solution by H_2O_2/Fe^{2+}, H_2O_2/Fe^{3+}, Fe (VI) and UV, H_2O_2/UV, $K_2S_2O_8$/UV. *Chemical Engineering Journaly*, **241**, 504-512. https://doi.org/10.1016/j.cej.2013.10.036

[26] Kazemifard, A.G., Moore, D.E. and Aghazadeh-Habashi, A. (2001) Identification and Quantitation of Sodium-Thyroxine and Its Degradation Products by LC Using Electrochemical and MS Detection. *Journal of Pharmaceutical and Biomedical Analysis*, **25**, 697-711. https://doi.org/10.1016/S0731-7085(01)00370-3

[27] Chen, B.Y., Lee, W. and Westerhoff, P.K. (2010) Solar Photolysis Kinetics of Disinfection Byproducts. *Water Research*, **44**, 3401-3409. https://doi.org/10.1016/j.watres.2010.03.014

[28] Sprehe, M., Geißen, S.U. and Vogelpohl, A. (2001) Photochemical Oxidation of Iodized X-Ray Contrast Media (XRC) in Hospital Wastewater. *Water Science and Technology*, **44**, 317-323. https://doi.org/10.2166/wst.2001.0315

[29] Gu, Y., Han, Q. and Dong, Z. (2022) Enhanced Degradation and Deiodination of Diatrizoate in a Sulfite Mediated Photolytic System: Performance, Products and Possible Pathways. *Journal of Hazardous Materials Advances*, **8**, Article 100144. https://doi.org/10.1016/j.hazadv.2022.100144

[30] Ye, T., Zhang, T.Y. and Tian, F.X. (2021) The Fate and Transformation of Iodine Species in UV Irradiation and UV-Based Advanced Oxidation Processes. *Water Re-*

search, **206**, Article 11775. https://doi.org/10.1016/j.watres.2021.117755

[31] Wei, Y.J., Liu, C.G. and Mo, L.P. (2005) Ultraviolet Absorption Spectra of Iodine, Iodide Ion and Triiodide Ion. *Spectroscopy and Spectral Analysis*, **25**, 86-88.